The simulation of debris particle sedimentation and formation in Severe Accident using the CFD-DEM algorithm: Preliminary Results

Byoungcheol Hwang [a], Eunho Kim [a], Hyun Sun Park [a*]
[a]*Division of Advanced Nuclear Engineering, POSTECH, Hyoja-dong, Nam-gu, Pohang, Kyung-buk, South Korea*
[*]*Corresponding author: hejsunny@postech.ac.kr*

1. Introduction

In Severe Accident of nuclear power plant, the cooling of corium is the most important performance. In case of ex-vessel cooling that the corium penetrates the reactor pressure vessel and falls into the cavity, there are several strategies for cooling down the corium temperature [1]. In Korea, the flooding cavity strategy is accepted, so the corium is solidified into debris particles and settled in to the cavity bottom. The formation of particle settlement may be flat or heap-like shape, and this factor has an effect on the whole cooling mechanism including flow path of coolant, natural circulation of surrounding part, and so on [2,3]. Also, it is hard to investigate the settlement process by experiment because of size limit and test condition. In this paper, the numerical approach for debris particle sedimentation phenomenon was suggested using the CFD-DEM (Computational Fluid Dynamics-Discrete Element Method) algorithm [4]. The code validation was achieved by comparing experimental cases [2] such as particle bed height, repose angle and so on.

2. Methods and Results

In this section, the basic algorithm of CFD-DEM and DAVINCI experiment facility are described. The code is actively under development while validating with experimental results. The numerical simulation of DAVINCI experiments were performed and analyzed by comparing bed height and repose angle.

2.1 The CFD-DEM Algorithm

CFD-DEM, the coupling of Computational Fluid Dynamics (CFD) and Discrete Element Method (DEM), was developed for simulating fluid-solid interaction. In CFD region using Eulerian method, each mesh point calculates data such as coordinate, velocity, pressure by solving Navier-Stokes equation. DEM which was proposed by Cundall et al. [5] calculates the interaction of many particles using Lagrangian method. It simplifies the contact force between two particles into spring and damping structure, so the movement of particles can be calculated efficiently.

The coupling process between CFD and DEM can be achieved through the exchange of solid-fluid interaction term. At first, DEM solver calculates one-step to transfer particle position and velocity data. Then CFD recognize individual particle's data in each cell. Then, the mean particle velocity is calculated in each cell. Using this value, the momentum exchange term and fluid flow are calculated in CFD region. Finally, the force term on each particle by fluid flow is calculated and transferred to DEM solver. The whole algorithm of CFD-DEM is shown in Figure 1.

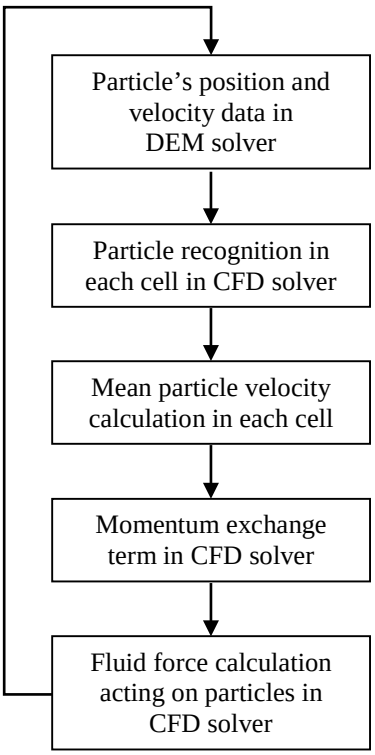

Fig. 1. The whole algorithm of CFD-DEM

The governing equation of DEM consists of three components: normal and tangential contact force ($\boldsymbol{F}_i^n$ and $\boldsymbol{F}_i^t$) with other particles, the force by fluid regime ($\boldsymbol{F}_i^f$), and gravity ($\boldsymbol{F}_i^g$). Those equations are shown in below for a particle *i*.

$$\sum \boldsymbol{F}_i = \boldsymbol{F}_i^n + \boldsymbol{F}_i^t + \boldsymbol{F}_i^f + \boldsymbol{F}_i^g \quad (1)$$

$$\boldsymbol{I}_i \frac{d\boldsymbol{\omega}_i}{dt} = \boldsymbol{r}_i^c \times \boldsymbol{F}_i^t + \boldsymbol{T}_i \quad (2)$$

$\boldsymbol{F}_i^n$ and $\boldsymbol{F}_i^t$ follow Hertzian or Hooke contact theory [5]. $\boldsymbol{F}_i^f$ can contain buoyancy force, drag force, virtual mass force, Basset force, lift force and so on. In this research, only the buoyancy and drag forces are considered

because of the low Reynolds regime. $\boldsymbol{F}_i^g$ is the body force, and eq.(2) shows the rotational force balance. $\boldsymbol{I}_i$ is the identity matrix and ω is the angular velocity of particle *i*. $\boldsymbol{r}_i^c$ and $\boldsymbol{T}_i$ are the contact radius and torque of particle *i*.

$$\frac{\partial(\rho_f \varepsilon)}{\partial t} + \nabla \cdot \left(\rho_f \varepsilon \boldsymbol{u}_f\right) = 0 \tag{3}$$

$$\frac{\partial(\rho_f \varepsilon \boldsymbol{u}_f)}{\partial t} + \nabla \cdot \left(\rho_f \varepsilon \boldsymbol{u}_f \boldsymbol{u}_f\right) = -\varepsilon \nabla p + \varepsilon \nabla \cdot (\mu \nabla \boldsymbol{u}_f) + \boldsymbol{R}_{f,p} + \varepsilon \rho_f g \tag{4}$$

The volume-averaged Navier-Stokes equations are included in governing equation in CFD part. ρ_f is fluid density and ε is the volume fraction of fluid phase in the cell. $\boldsymbol{u}_f$, p, and μ are the average velocity, pressure, and viscosity of fluid part. $\boldsymbol{R}_{f,p}$ is the momentum exchange term derived from the solid motion, and it is the function of solid-fluid interaction term ($\boldsymbol{F}_i^f$), fluid velocity ($\boldsymbol{u}_f$), and particle mean velocity ($\langle \boldsymbol{u}_p \rangle$). $\boldsymbol{F}_i^f$ is the sum of drag force and buoyancy force (eq.(6)).

$$\boldsymbol{R}_{f,p} = -\frac{\left|\sum \boldsymbol{F}_i^f\right|}{V_{cell}\left|\boldsymbol{u}_f - \langle \boldsymbol{u}_p \rangle\right|}\left(\boldsymbol{u}_f - \langle \boldsymbol{u}_p \rangle\right) \tag{5}$$

$$\sum \boldsymbol{F}_i^f = \boldsymbol{F}_i^D + \boldsymbol{F}_i^B \tag{6}$$

$$\boldsymbol{F}_i^D = \frac{1}{8} C_d \rho_f \pi {d_p}^2 \left(\boldsymbol{u}_f - \langle \boldsymbol{u}_p \rangle\right)\left|\boldsymbol{u}_f - \langle \boldsymbol{u}_p \rangle\right| \varepsilon^{1-\chi} \tag{7}$$

$$C_d = \left(0.63 + \frac{4.8}{Re^{\frac{1}{2}}}\right)^2 \tag{8}$$

$$Re = \frac{\varepsilon \rho_f \left|\boldsymbol{u}_f - \langle \boldsymbol{u}_p \rangle\right|}{\mu} \tag{9}$$

$$\chi = 3.7 - 0.65 \exp\left(-\frac{(1.5 - log_{10} Re)^2}{2}\right) \tag{10}$$

$$\boldsymbol{F}_i^B = \rho_f g V_p = \frac{1}{6} \rho_f g \pi {d_p}^3 \tag{11}$$

In this research, the correlation of drag force developed by Di Felice [6] was used, and the related parameters are shown from eq.(7) to eq.(10). C_d is drag coefficient, d_p is the particle diameter, and Re is Reynolds number. Buoyancy force is not negligible in water, so the force derived by particle volume (V_p) and liquid density (ρ_f) was used in eq.(11). For the simulation of experimental cases, the open-source code, CFDEM®coupling was used [7]. It couples LIGGGHTS (LAMMPS Improved for General Granular and Granular Heat Transfer Simulations) [8] for DEM and OpenFOAM (Open Source Field Operation And Manipulation) for CFD, so the simulation of massive particles in fluid region is available.

2.2 Experimental Cases (DAVINCI)

The simulation target is the DAVINCI experiment [2]. The objective of this experiment is the investigation of the two-phase flow effect on the debris particle sedimentation process in Severe Accident. Figure 2 shows the schematic diagram of experimental facility. The facility height is 1000mm and the diameter of particle catcher plate is 600mm. Water is filled up to 760mm height and the funnel which has 14.5mm inner diameter is located 95mm above on the free surface. Stainless steel 304 (ρ=8000kg/m^3) was used for simulant particle and it has cylindrical shape with 2mm diameter and 2mm height. Quiescent pool condition (w/o air) and two-phase condition (w/ air) were performed having 10s time sequence for comparing the two-phase flow effect. The result data is the overall shape formation on various viewpoint, top height of the bed, repose angle, and so on. Only the data of quiescent pool condition was used for the code validation in this research. Also, other data on these experimental data can be used supportive data for numerical code validation or the basis of phenomenological modelling. More detailed information is described in reference paper [2].

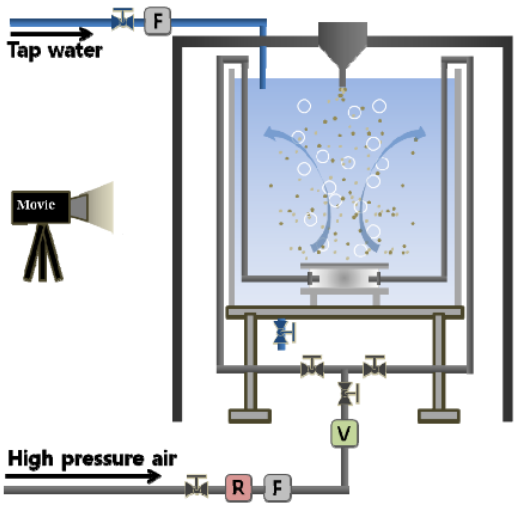

Fig. 2.The schematic diagram of experimental facility (DAVINCI) [2]

2.3 Simulation Results and Discussion

Some material properties and multi-time step algorithm should be considered for the simulation At first, the physical properties such as density, Young's modulus, Poisson's ratio of the simulant particle (stainless steel 304) are used for input information on DEM. Also some coefficient such as particle-particle & particle-wall friction coefficient, coefficient of restitution (COR), and rolling friction coefficient should be defined by considering geometrical effect or circumstance. Those properties are shown in below Table I. Second, the time step of DEM calculation should be small enough (about 10^{-6}s) to get a stability. If the time step of both CFD and DEM is 10^{-6}, the computational time cost will be

enormous, so the multi-time step algorithm is applied. For example, if the time step is 10^{-6} on DEM and 10^{-4} on CFD, 100 calculations of DEM is coupled with 1 calculation of CFD. Then, the time computation can be reduced and also the stability of DEM is achieved. The time step information is also shown in Table I.

The calculation was performed like Figure 3, and the whole time cost was 14hrs using 16GB RAM, 8CPU parallel computation. The total number of particles is 19894, and 6240 meshes are used in CFD. The data results comparing with experiment is the overall view, particle bed height and repose angle.

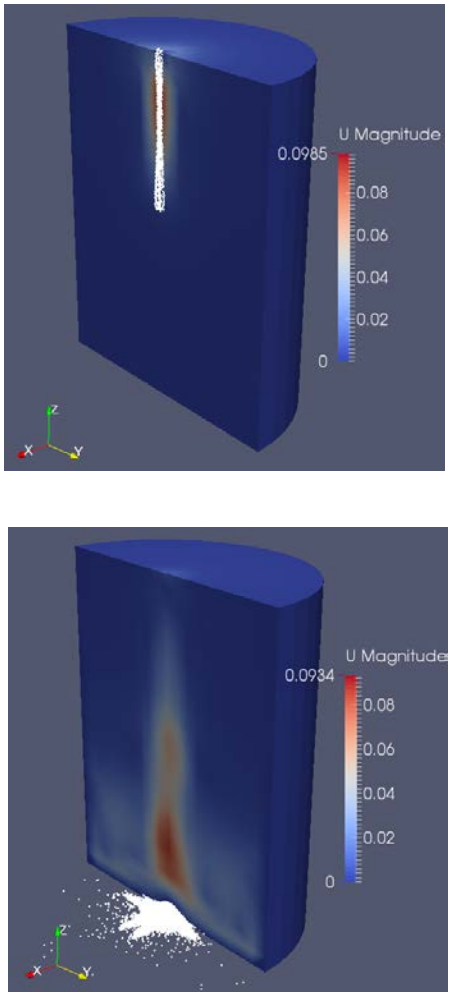

Fig. 3. The numerical simulation of the DAVINCI experiment using CFDEM with liquid velocity (m/s): 0.5s case (upper), 13s case (lower)

Table I: Physical properties and time step conditions

Physical properties (Stainless Steel 304)	
Density [kg/m^3]	8000
Young's modulus [GPa]	200
Poisson's ratio	0.29
Friction coefficient (particle-particle)	0.7
Friction coefficient (particle-wall)	0.7
Coefficient of restitution	0.7
Rolling friction coefficient	0.1
Time step [s]	
DEM	10^{-6}
CFD	10^{-4}
End time	13

The overall view of experimental and numerical data is shown in Figure 4~6. First, the inclined view, the less particles were dispersed in simulation cases than experiment. In Figure 5, the less particle dispersion can be seen more accurately in top view. The degree of particle dispersion is depend on the friction coefficient and rolling friction coefficient which were defined by user, so the sensitivity test for these parameters should be analyzed in the future. Also, the specific path of particle movement is shown in numerical case (Fig.5), and this phenomenon is occurred by the mesh dependency.

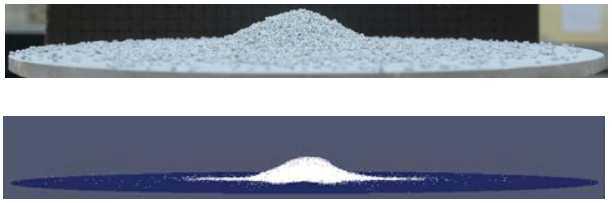

Fig. 4. Inclined view of particle bed formation: experiment (upper), simulation (lower)

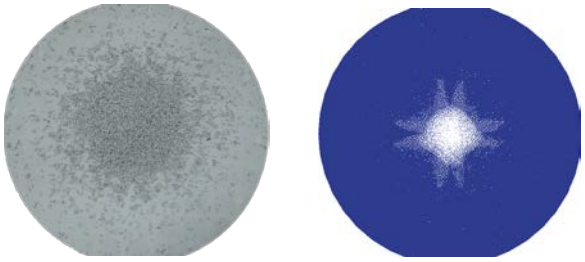

Fig. 5. Top view of particle bed formation: experiment (left), simulation (right)

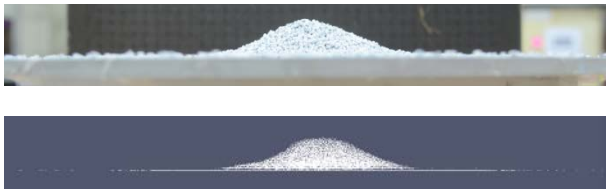

Fig. 6. Side view of particle bed formation: experiment (upper), simulation (lower)

The quantified comparison is available through the side view (Figure 6). The height (H) and repose angle (θ) of particle bed can be defined using the assumption that the bed configuration is ideal cone shape shown in Figure 7. Table II shows the comparison results of measured data and the error is about 11~14%. The particle bed shape in simulation is little more flat and it means that stronger particle-particle effect is needed for more accurate calculation.

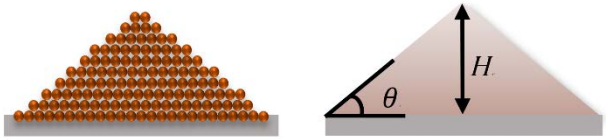

Fig. 7. The definition of particle bed height (H) and repose angle (θ)

Table II: The comparison of experiment and simulation data

	Experiment	Simulation	Error [%]
H [mm]	28.2	24.2	14.2
θ [°]	23.9	21.2	11.3

3. Conclusions

In this research, the approach of numerical simulation using CFD-DEM algorithm was applied to analyze the particle settlement and formation. The code validation for solid-liquid interaction was performed and some differences in the overall view was shown by the sensitivity of physical properties which should be investigated. The results of the particle bed height and repose angle is similar with experimental cases. This numerical approach can have the capacity to simulate two-phase interaction and thermal hydraulic mechanism, so it will be an important key for analyzing ex-vessel Severe Accident phenomena.

ACKNOWLEDGEMENT

This research was supported by Nuclear Safety Research Program of the Korea Radiation Safety Foundation grants funded by Korean government (NSSC) (Grant Code: 1305008-0113-HD140).

REFERENCES

[1] B. R. Seghal, “Nuclear Safety in Light Water Reactors: Severe Accident Phenomenology”, Elsevier, 2012.
[2] E. Kim, M. Lee, H. S. Park, J. H. Park, Experimental Study on the Ex-Vessel Corium Debris Bed Development under Two-Phase Natural Convection Flows in Flooded Cavity Pool, The 7th European Review Meeting on Severe Accident Research (ERMSAR-2015), 2015-032, 2015.
[3] S. E. Yakush, P. Kudinov and T. N. Dinh, Multiscale Simulations of Self-organization Phenomena in the Formation and Coolability of Corium Debris Bed, NURETH-13, N13P1143, 2009.
[4] C. Goniva, C. Kloss, N. G. Deen, J.A.M. Kuipers and S. Pirker, Influence of Rolling Friction Modelling on Single Spout Fluidized Bed Simulations, Particuology, **10**, 582-591, DOI 10.1016/j.partic.2012.05.002, 2012.
[5] P. A. Cundall and O. D. Strack, A discrete numerical model for granular assemblies, Geotechnique, **29**, No.1, 47–65, 1979.
[6] R. Di Felice, The voidage function for fluid–particle interaction systems, International Journal of Multiphase Flow, **20**, No.1, 153–159, 1994.
[7] C. Goniva, C. Kloss, A. Hager, S. Pirker, An open source CFD–DEM perspective, Proc. of the 5th OpenFOAM Workshop, June 22-24, (Göteborg), 2010.
[8] C. Kloss, C. Goniva, LIGGGHTS: a new open source discrete element simulation software, Proc. 5th Int. Conf. on Discrete Element Methods, London, UK, Aug, 2010.